Chemical Science

EDGE ARTICLE

View Article Online
View Journal | View Issue

Cite this: *Chem. Sci.*, 2015, **6**, 2968

Expanding discriminative dimensions for analysis and imaging†‡

Jérôme Querard,[abc] Arnaud Gautier,*[abc] Thomas Le Saux*[abc] and Ludovic Jullien*[abc]

Eliminating the contribution of interfering compounds is a key step in chemical analysis. In complex media, one possible approach is to perform a preliminary separation. However purification is often demanding, long, and costly; it may also considerably alter the properties of interacting components of the mixture (*e.g.* in a living cell). Hence there is a strong interest for developing separation-free non-invasive analytical protocols. Using photoswitchable probes as labelling and titration contrast agents, we demonstrate that the association of a modulated monochromatic light excitation with a kinetic filtering of the overall observable is much more attractive than constant excitation to read-out the contribution from a target probe under adverse conditions. An extensive theoretical framework enabled us to optimize the out-of-phase concentration first-order response of a photoswitchable probe to modulated illumination by appropriately matching the average light intensity and the radial frequency of the light modulation to the probe dynamics. Thus, we can selectively and quantitatively extract from an overall signal the contribution from a target photoswitchable probe within a mixture of species, photoswitchable or not. This simple titration strategy is more specifically developed in the context of fluorescence imaging, which offers promising perspectives.

Received 19th December 2014
Accepted 18th February 2015

DOI: 10.1039/c4sc03955f

www.rsc.org/chemicalscience

Introduction

One of the main challenges for chemists remains being able to quantify a specific analyte in highly complex systems such as biological or medical samples.[1–3] A crude sample (*e.g.* cell extract), like those found in diagnostics assays,[4] drug screening,[5,6] or metabolites quantification,[7] may contain up to 10^4 to 10^5 rather similar components at concentrations covering ten orders of magnitude. Analysis requires in general challenging sample conditioning and preliminary purifications. Selective detection is even more challenging when the sample has to remain in its native state (*e.g.* living cells). Non-invasive methods have thus to be adopted. The archetype of such methods is fluorescence microscopy, which has revolutionised the way one observes biological samples.[8,9] However relying on fluorescence as read-out presents several limitations. Hence multiplexed observations of more than a few fluorescent species are difficult because of spectral crowding resulting from the large emission bandwidth of most fluorophores. Moreover biological media often produce high levels of scattering and autofluorescence at optical wavelengths, which interfere with the signals of interest and diminish the contrast. There is therefore a strong need for approaches enabling to circumvent the selectivity issue in the context of both analysis and imaging.

To detect a target in a complex medium, one needs a probe. This probe can be intrinsic, *i.e.* present in the target (atoms or functional groups). However it is often difficult to find an intrinsic probe that is unique for a target. For instance, biomolecules (*e.g.* proteins, nucleic acids) are essentially composed of the same functionalities. Alternatively, exogenous probes with unnatural chemical functions or singular spectroscopic properties can be used to give a unique signature and act as contrast agents. Additional selectivity can be observed if the exogenous probe is engaged in a reactive process. This is typically the strategy of titration experiments, where one observes a reagent specifically probing the analyte of interest thanks to a chemical reaction. Selectivity classically results from the difference between the equilibrium constants associated to the titration reaction. Relying on kinetics[10] opens further dimensions to improve selectivity by increasing the number of discriminating parameters: in the most simple case, *two* independent rate constants instead of only *one* thermodynamic constant are associated to the titration reaction for each system component. In this account, we exploit chemical kinetics to introduce a simple and cheap protocol for selective analysis or

[a]*Ecole Normale Supérieure-PSL Research University, Département de Chimie, 24, rue Lhomond, F-75005 Paris, France. E-mail: Arnaud.Gautier@ens.fr; Thomas.Lesaux@ens.fr; Ludovic.Jullien@ens.fr; Tel: +33 4432 3333*

[b]*Sorbonne Universités, UPMC Univ Paris 06, PASTEUR, F-75005, Paris, France*

[c]*CNRS, UMR 8640 PASTEUR, F-75005, Paris, France*

† This article is dedicated to Prof. Manfred Eigen.

‡ Electronic supplementary information (ESI) available: Reduction of photo-(physical)chemical mechanisms to a two-state exchange, kinetic analysis of the two-state model, retrieval of concentrations from the observables, improvement of the spatial resolution. See DOI: 10.1039/c4sc03955f

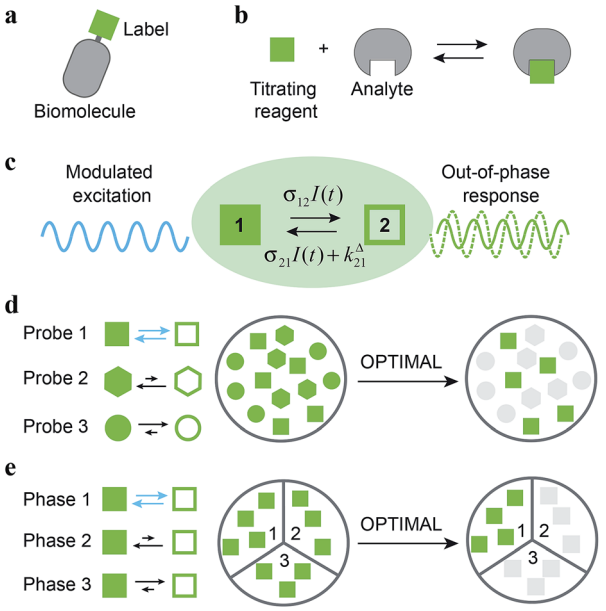

Fig. 1 Out-of-Phase TItration after Modulation of Activating Light (OPTIMAL) for selective detection of a photoswitchable probe. When illuminated, a photoswitchable probe (green square) used either (a) as a label or (b) as a titrating reagent exchanges between two distinguishable states **1** and **2** (c). With a periodic modulated light, its response signal is modulated with a phase shift. The amplitude of the out-of-phase (or quadrature-delayed) first-order component of its response is optimal when the average intensity and the angular frequency of the modulated light match the dynamic parameters of the probe. Accordingly, when the modulated light is tuned to its dynamics, the photoswitchable probe is the only species giving a significant signal in quadrature detection. This enables its selective detection in (d) a mixture of interfering probes or species displaying different dynamics or, if its dynamics is environment-sensitive, in (e) a specific phase of a heterogeneous multiphasic medium.

imaging of a probe used either as a label (Fig. 1a) or as a titrating reagent (Fig. 1b).

Kinetic information can be uncovered by relaxation methods,[11] where an externally driven excitation forces the system out-of-equilibrium.[12–17] Recently, selective imaging protocols relying on kinetic filtering have been implemented upon modulating the probe signal using light[18–31] or temperature[32–34] as external triggers. In this work, we adopted light as a non-invasive and easily modulatable trigger. We additionally chose photo-switchable probes, which interconvert between two states upon light illumination and correspondingly exhibit several discriminating parameters that can be used to optimize an efficient dynamic contrast (Fig. 1c).[35] As we already showed in the context of selective analysis and separation,[32,34,36–38] modulation of a control parameter can reveal intrinsic chemical kinetics upon periodically forcing the system out-of-equilibrium. By analogy, we adopted a periodically oscillating monochromatic light excitation, which modulates the extent of the photochemical reaction, thereby modulating the reporting signal. Beyond favoring discrimination against background noise by means of a lock-in detection[39] such a modulation enables subsequent kinetic filtering. More precisely, we show theoretically how tuning both the average intensity and the frequency of the modulated monochromatic light excitation permits to simply and selectively extract from the overall signal the contribution from a photoswitchable probe of interest within a mixture of species, photoswitchable or not. Hence it will be possible to specifically retrieve the contribution from a targeted probe in a mixture of interfering probes (Fig. 1d), or the contribution originating from a specific compartment when a medium-sensitive probe is incorporated in a heterogeneous multiphasic medium (Fig. 1e). We correspondingly dubbed our approach OPTIMAL for Out-of-Phase TItration after Modulation of Activating Light. In particular, it generalizes the fluorescence imaging approach OPIOM (Out-of-Phase Imaging after Optical Modulation) we recently introduced,[40] which enables selective and quantitative imaging of photoswitchable fluorescent proteins.

Optimizing the response of a photoswitchable probe to periodic illumination

The model

The dynamic behavior of a photoswitchable probe **P** illuminated with a light of intensity $I(t)$ can be described by the two-state exchange (1)

$$\mathbf{1} \underset{k_{21}(t)}{\overset{k_{12}(t)}{\rightleftharpoons}} \mathbf{2} \quad (1)$$

where the thermodynamically more stable state **1** is photochemically converted to the thermodynamically less stable state **2** at rate constant

$$k_{12}(t) = \sigma_{12} I(t), \quad (2)$$

from which it can relax back to the initial state **1** either by a photochemically- or a thermally-driven process at rate constant

$$k_{21}(t) = \sigma_{21} I(t) + k_{21}^{\Delta}, \quad (3)$$

where $\sigma_{21}I(t)$ and k_{21}^{Δ} are respectively the photochemical and the thermal contributions of the rate constant. In that case, the molecular action cross-sections for photoisomerization σ_{12} and σ_{21} and the thermal rate constant k_{21}^{Δ} fully define the behavior of the photoswitchable probe.

It is worth to mention that the following theoretical development involving a truncation of the kinetic equations to various orders of the light intensity could be applied to other mechanisms possibly involving non-linearities. However the scheme (1) provides simple expressions. Furthermore it is already relevant to model several multi-step mechanisms, which can be dynamically reduced to light-driven exchanges between two states.[41–43] Hence, in ESI,† we first demonstrate that this scheme satisfactorily accounts for the behavior of photochromic probes. Then we show that it describes as well the dynamics of (i) a chromophore yielding singlet and triplet states upon illuminating and (ii) a photoswitchable probe sensing an analyte present in excess as long as photochemical steps are rate-limiting.

Concentration response to constant illumination

When the system is submitted to a constant illumination defined by the intensity $I(t) = I^0$, the forward and backward rate constants become

$$k_{12}(t) = k_{12}^0 = \sigma_{12} I^0 \tag{4}$$

$$k_{21}(t) = k_{21}^0 = \sigma_{21} I^0 + k_{21}^{\Delta}. \tag{5}$$

After a transient regime defined by the relaxation time $\tau_{12}^0 = 1/(k_{12}^0 + k_{21}^0)$, the system reaches a photostationary state characterized by the apparent photoisomerization constant $K_{12}^0 = k_{12}^0/k_{21}^0$. The concentrations of **1** and **2**, noted respectively 1^0 and 2^0, are then given by

$$1^0 = P_{\text{tot}} - 2^0 = \frac{1}{1 + K_{12}^0} P_{\text{tot}} \tag{6}$$

where P_{tot} is the total concentration of **P**.

Concentration response to sinusoidal modulation of small amplitude

To evaluate the behavior of such system upon illumination with a periodically modulated light, we first consider a sinusoidally modulated illumination oscillating around the averaged value I^0 at angular frequency ω and with a small amplitude εI^0 ($\varepsilon \ll 1$) such that

$$I(t) = I^0[1 + \varepsilon \sin(\omega t)]. \tag{7}$$

Temporal dependence of the concentrations. After introducing the expression (7) into eqn (2) and (3), the system of differential equations governing the temporal evolution of the concentrations in **1** and **2** is solved at the first-order expansion in the light perturbation (see ESI†). Beyond the relaxation time τ_{12}^0, one enters into the forced and permanent regime where the concentration $i = i^0 + \varepsilon i^1(t)$ in each species **i** (**i** = **1** or **2**) oscillates around a mean value i^0 (corresponding to the concentration of **i** at steady-state associated to the photon flux I^0; see eqn (6)) at the angular frequency ω but with a phase delay of $\phi_{12} = \arctan(\omega\tau_{12}^0)$

$$2^1(t) = -1^1(t) = \frac{\rho_{12}^0 \tau_{12}^0 p_{21}^{\Delta}}{\sqrt{1 + (\omega\tau_{12}^0)^2}} \sin(\omega t - \phi_{12}). \tag{8}$$

In eqn (8), $\rho_{12}^0 = k_{12}^0 1^0 = k_{21}^0 2^0$ and $p_{21}^{\Delta} = k_{21}^{\Delta}/(\sigma_{21} I^0 + k_{21}^{\Delta})$ respectively designate the steady-state rate of reaction (1) and the relative thermal contribution to the relaxation of state **2** upon illuminating at I^0.

The phase-delayed oscillating concentrations i can also be written

$$i(t) = i^0 + \varepsilon[i^{1,\text{in}} \sin(\omega t) + i^{1,\text{out}} \cos(\omega t)] \tag{9}$$

where $\varepsilon i^{1,\text{in}} \sin(\omega t)$ and $\varepsilon i^{1,\text{out}} \cos(\omega t)$ are in-phase and out-of-phase (or quadrature-delayed) oscillating terms at angular frequency ω. The amplitudes $i^{1,\text{in}}$ and $i^{1,\text{out}}$ of the in-phase and out-of-phase oscillating terms are (see ESI†)

$$2^{1,\text{in}} = -1^{1,\text{in}} = \rho_{12}^0 \tau_{12}^0 p_{21}^{\Delta} \frac{1}{1 + (\omega\tau_{12}^0)^2} \tag{10}$$

$$2^{1,\text{out}} = -1^{1,\text{out}} = -\rho_{12}^0 \tau_{12}^0 p_{21}^{\Delta} \frac{\omega\tau_{12}^0}{1 + (\omega\tau_{12}^0)^2} \tag{11}$$

or similarly

$$2^{1,\text{in}} = -1^{1,\text{in}} = p_{21}^{\Delta} \frac{K_{12}^0}{(1 + K_{12}^0)^2} \frac{1}{1 + (\omega\tau_{12}^0)^2} P_{\text{tot}} \tag{12}$$

$$2^{1,\text{out}} = -1^{1,\text{out}} = -p_{21}^{\Delta} \frac{K_{12}^0}{(1 + K_{12}^0)^2} \frac{\omega\tau_{12}^0}{1 + (\omega\tau_{12}^0)^2} P_{\text{tot}} \tag{13}$$

to make explicit the proportionality of $2^{1,\text{in}}$ and $2^{1,\text{out}}$ with the total **P** concentration.

Optimal out-of-phase response. Fig. 2a and b displays the dependence of the normalized in-phase $|1_{\text{norm}}^{1,\text{in}}| = |1^{1,\text{in}}/P_{\text{tot}}|$ and out-of-phase $|1_{\text{norm}}^{1,\text{out}}| = |1^{1,\text{out}}/P_{\text{tot}}|$ amplitudes on the control parameters I^0 and ω for a given photoswitchable probe **P** characterized by the triplet of parameters (σ_{12}, σ_{21}, k_{21}^{Δ}). In contrast to the in-phase amplitude, the out-of-phase amplitude exhibits a single optimum when the control parameters (I^0, ω) verify

$$I^0 = \frac{k_{21}^{\Delta}}{\sigma_{12} + \sigma_{21}} \tag{14}$$

$$\omega = 2k_{21}^{\Delta} \tag{15}$$

with full widths at half-maximum $4\sqrt{2}k_{21}^{\Delta}/(\sigma_{12} + \sigma_{21})$ along I^0 and $4\sqrt{3}k_{21}^{\Delta}$ along ω. The normalized out-of phase amplitude $|1_{\text{norm}}^{1,\text{out}}|$ is then equal to $\sigma_{12}/[8(\sigma_{12} + \sigma_{21})]$.

The optimization of $1^{1,\text{out}}$ results from the independent optimisation of the terms $p_{21}^{\Delta} K_{12}^0 P_{\text{tot}}/(1 + K_{12}^0)^2$ and $\omega\tau_{12}^0/[1 + (\omega\tau_{12}^0)^2]$ in eqn (13). From the expression (6) using eqn (4) and (5), one can calculate $d2^0/d \ln I^0$ to show that $\varepsilon p_{21}^{\Delta} K_{12}^0 P_{\text{tot}}/(1 + K_{12}^0)^2$ measures the composition shift $\delta 2^0$ from the steady-state 2^0 after a light intensity jump of amplitude εI^0. It depends on I^0 and is maximized in a regime of intermediate illumination, in which thermally- and photochemically-driven reactions occur at the same rate such that $k_{21}^{\Delta} = (\sigma_{12} + \sigma_{21}) I^0$ (see eqn (14)). When the light intensity is too low, the thermal relaxation dominates the photoisomerization and the light intensity jump εI^0 cannot significantly shifts the photoswitchable probe from the state **1**. Conversely, when the light intensity is too large, the thermal relaxation does not contribute anymore to the dynamics of the exchange (1): the relative proportions in states **1** and **2** become independent of the light intensity, so there is no composition shift induced by the light jump. The second optimized term, $\omega\tau_{12}^0/[1 + (\omega\tau_{12}^0)^2]$, is maximized upon matching the radial frequency of the light modulation ω with the exchange relaxation time τ_{12}^0 so that $\omega\tau_{12}^0 = 1$ (see eqn (14) and (15)). When $\omega \gg 1/\tau_{12}^0$, the exchange is slow compared to the light variations and the couple {**1**, **2**} has not enough time to respond: both $i^{1,\text{in}}$ and

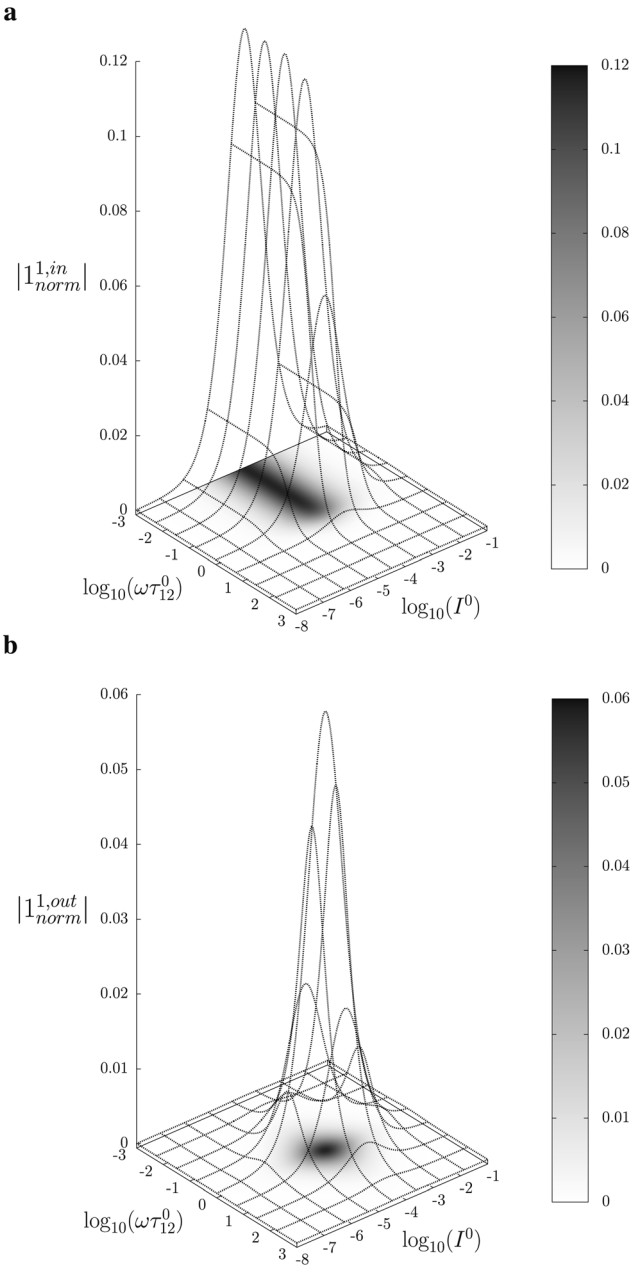

Fig. 2 Theoretical computation of the response of a photoswitchable fluorophore **1** ⇌ **2** submitted to light harmonic forcing of small amplitude. The absolute values of the normalized amplitudes of the in-phase and out-of-phase oscillations in **1** concentration, $|1^{1,in}_{norm}|$ (a) and $|1^{1,out}_{norm}|$ (b) respectively, are plotted *versus* the light flux I^0 (in ein s^{-1} m^{-2}) and the adimensional relaxation time $\omega\tau^0_{12}$. $\sigma_{12} = 73$ m^2 mol^{-1}, $\sigma_{21} = 84$ m^2 mol^{-1}, $k^{\Delta}_{21} = 1.5 \times 10^{-2}$ s^{-1}. See eqn (12) and (13).

$i^{1,out}$ vanish. Conversely, when $\omega \ll 1/\tau^0_{12}$, $i^{1,out}$ cancels, so the concentrations of **1** and **2** oscillate in phase with the light modulation.

Concentration response to square wave modulation of small amplitude

As an experimentally relevant extension of the previous case, we analyzed the behavior of the system upon illumination with a square wave light modulation of weak amplitude around the averaged value I^0. We adopted its Fourier series expansion

$$I(t) = I^0\left[1 + \frac{4\varepsilon}{\pi}\sum_{p=0}^{\infty}\frac{1}{2p+1}\sin[(2p+1)\omega t]\right] \qquad (16)$$

with $\varepsilon \ll 1$ upon choosing the starting time ($t = 0$) halfway through the first pulse.

Temporal dependence of the concentrations. The expression (16) was introduced into eqn (2) and (3) and the system of differential equations governing the temporal evolution of the concentrations in **1** and **2** was again solved at the first-order expansion in the light perturbation (see ESI†). In the forced and permanent regime observed beyond the relaxation time τ^0_{12}, the concentration i in each species **i** (**i** = **1** or **2**) now oscillates around i^0 at multiple angular frequencies $(2p + 1)\omega$

$$i(t) = i^0 + \varepsilon\sum_{p=0}^{\infty}\left[i^{1,in}_{(2p+1)}\sin[(2p+1)\omega t] + i^{1,out}_{(2p+1)}\cos[(2p+1)\omega t]\right] \qquad (17)$$

where the amplitudes of the in-phase and out-of-phase oscillating terms at angular frequency $(2p + 1)\omega$ are (see ESI†)

$$2^{1,in}_{(2p+1)} = -1^{1,in}_{(2p+1)} = \frac{4}{\pi}\frac{\rho^0_{12}\tau^0_{12}p^{\Delta}_{21}}{2p+1}\frac{1}{1+(2p+1)^2(\omega\tau^0_{12})^2} \qquad (18)$$

$$2^{1,out}_{(2p+1)} = -1^{1,out}_{(2p+1)} = -\frac{4}{\pi}\frac{\rho^0_{12}\tau^0_{12}p^{\Delta}_{21}}{2p+1}\frac{(2p+1)\omega\tau^0_{12}}{1+(2p+1)^2(\omega\tau^0_{12})^2}. \qquad (19)$$

Except for the numerical factor $4/\pi$, the expressions (10), (11) and (18), (19) for $p = 0$ are similar. This observation suggests that the resonance conditions (14) and (15) valid for the optimization of $1^{1,out}$ with the weak sinusoidal light modulation at radial frequency ω are equally relevant to optimize the amplitude $1^{1,out}_{(1)}$ when the system is submitted to a weak square wave light modulation of fundamental radial frequency ω. In fact, this conclusion would equally apply for any periodic light modulation of small amplitude with fundamental radial frequency ω. Indeed, at first order, the amplitude of the out-of-phase modulation of the concentrations of the species **1** and **2** at radial frequency ω only originates from the sinusoidal modulation at radial frequency ω in the Fourier series associated to the light modulation.

Concentration response to periodic modulations of large amplitude

The use of a modulation of small amplitude is favorable to derive simple analytical expressions. However, it generates only small variations of the probe signal because of the small modulation, which is a drawback to reliably extract the out-of-phase amplitude of the first order response from the experimental signal. To overcome this limitation, we analyzed the response of a photoswitchable probe to the preceding periodic illuminations but with a large modulation amplitude α. Thus we adopted

$$I(t) = I^0[1 + \alpha \sin(\omega t)] \quad (20)$$

and

$$I(t) = I^0\left\{1 + \frac{4\alpha}{\pi}\sum_{p=0}^{\infty}\frac{1}{2p+1}\sin[(2p+1)\omega t]\right\} \quad (21)$$

for the sinusoidal and square wave modulation respectively. In particular, the latter periodic illumination is of simple experimental implementation (on–off illumination switching).

Temporal dependence of the concentrations. The ESI† details the calculations referring to these two modulations of large amplitude. In this paragraph, we only introduce the calculation guideline, which is common to both types of modulations. The light intensity can be written

$$I(t) = I^0[1 + \alpha h(\omega t)] \quad (22)$$

where $h(\omega t)$ designate a periodic function with fundamental radial frequency ω. Eqn (22) was used to express the rate constants with eqn (2) and (3). Then, upon expanding the concentration expressions as

$$2 = 2^0 + \alpha f(\omega t) \quad (23)$$

$$1 = 1^0 - \alpha f(\omega t), \quad (24)$$

the system of differential equations governing the temporal evolution of the concentrations in **1** and **2** becomes

$$\frac{df(\theta x)}{dx} = -f(\theta x) + [a - bf(\theta x)]h(\theta x) \quad (25)$$

where

$$x = \frac{t}{\tau_{12}^0} \quad (26)$$

$$a = \rho_{12}^0 p_{21}^{\Delta}\tau_{12}^0 \quad (27)$$

$$b = \alpha(\sigma_{12} + \sigma_{21})I^0\tau_{12}^0 \quad (28)$$

$$\theta = \omega\tau_{12}^0. \quad (29)$$

Beyond the relaxation time τ_{12}^0, one enters into a permanent regime in which $f(\theta x)$ is a continuous periodic function. In contrast to the situation of light modulation of small amplitude, one cannot anymore restrict the $f(\theta x)$ analysis to the first-order. The $f(\theta x)$ function has to be expressed as a Fourier series

$$f(\theta x) = a_0 + \sum_{n=1}^{+\infty}[a_n \cos(n\theta x) + b_n \sin(n\theta x)] \quad (30)$$

where a_n and b_n designate the amplitudes of the n-th components of the Fourier series. The a_n and b_n terms can be extracted from eqn (25) upon identifying the amplitudes of the components of same order. Then one can obtain the expressions of the concentrations in **1** and **2**:

$$2 = 2^0 + \alpha\left\{a_0 + \sum_{n=1}^{+\infty}[a_n \cos(n\theta x) + b_n \sin(n\theta x)]\right\} \quad (31)$$

$$1 = 1^0 - \alpha\left\{a_0 + \sum_{n=1}^{+\infty}[a_n \cos(n\theta x) + b_n \sin(n\theta x)]\right\}. \quad (32)$$

Consequently, at steady-state, a large periodic modulation of illumination now causes modulation of the concentrations in **1** and **2** at an infinite number of radial frequencies. Eqn (31) and (32) can be transformed to explicit the amplitudes $\mathrm{i}^{n,in}$ and $\mathrm{i}^{n,out}$ of the in-phase and out-of phase terms oscillating at the radial frequency $n\omega$. The concentration of **i** can be now written

$$i = \mathrm{i}^{\circ} + \alpha\sum_{n=1}^{+\infty}\left[\mathrm{i}^{n,in}\sin(n\omega t) + \mathrm{i}^{n,out}\cos(n\omega t)\right]. \quad (33)$$

Interestingly, i°, $\mathrm{i}^{n,in}$ and $\mathrm{i}^{n,out}$ are proportional to P_{tot}. Indeed eqn (25) can be transformed into

$$\frac{df(\theta x)}{dx} + f(\theta x)[1 + bh(\theta x)] = ah(\theta x). \quad (34)$$

Neither b nor $h(\theta x)$ depend on P_{tot} (see eqn (20), (21) and (26–29)). In contrast, a is proportional to P_{tot} (see eqn (6) and (27)). Derivation being a linear operation, eqn (34) then implies that $f(\theta x)$ is proportional to P_{tot}. The system of equations giving access to a_n and b_n being linear (see ESI†), all the a_n and b_n amplitudes are individually proportional to P_{tot}. Finally, we use eqn (31–33) to deduce that i°, $\mathrm{i}^{n,in}$ and $\mathrm{i}^{n,out}$ are proportional to P_{tot}.

We showed that, in the case of light modulation of small amplitude, the out-of-phase amplitudes of the concentration modulation at radial frequency ω are optimal when the resonance conditions (14) and (15) are fulfilled. In the absence of analytical expressions for $\mathrm{1}^{1,out}$ and $\mathrm{2}^{1,out}$, such conclusions cannot be directly derived in the case of periodic light modulation of large amplitude. We correspondingly evaluated their relevance by means of numerical calculations (see ESI†). For harmonic forcing as well as square wave modulation in a regime of large amplitude modulation, we could show that $|\mathrm{1}_{norm}^{1,out}|$ exhibits an optimum in the space (I^0, ω), which position and amplitude are very close to those observed with a sinusoidal modulation of small amplitude. In fact, the error done when taking the analytical expression of the resonance conditions valid only for a modulation of small amplitude is always less than 20%, no matter which amplitude α is used. Such an error would be of the order of magnitude of the experimental errors done when fixing the average light intensity and radial frequency to their values at resonance, $I^{0,R}$ and ω^R.

Application to selective and quantitative detection of a photoswitchable probe

In the preceding section, we demonstrated that, for a photoswitchable probe submitted to a periodic modulated light, the out-of-phase first-order response of the concentration could be maximized by appropriately choosing both the average light

intensity and the radial frequency of the light modulation. However, in general, concentrations are retrieved from a signal. In this section, we analyze whether the out-of-phase response of the signal can be used for selective detection of a photoswitchable probe.

Out-of-phase response of the overall observable

The overall observable O (*e.g.* absorbance, electrophoretic mobility, …) from the photoswitchable probe results from the individual contributions of the states **1** and **2**. We assume that this observable varies linearly with the concentrations in **1** and **2**. We note Q_i the response factor of **i** linking signal and concentration (hereafter considered as constant). We can write

$$O(t) = Q_1 1(t) + Q_2 2(t). \tag{35}$$

In the general case of a periodic modulation of large amplitude, using the expressions of $1(t)$ and $2(t)$ given in eqn (33), the expression of the signal $O(t)$ becomes

$$O(t) = \mathfrak{O}^{\circ} + \sum_{n=1}^{\infty}\left[\mathfrak{O}^{n,\mathrm{in}} \sin(n\omega t) + \mathfrak{O}^{n,\mathrm{out}} \cos(n\omega t)\right], \tag{36}$$

where (see ESI†)

$$\mathfrak{O}^{1,\mathrm{out}} = (Q_2 - Q_1)\alpha 2^{1,\mathrm{out}}. \tag{37}$$

As shown in eqn (37), $\mathfrak{O}^{1,\mathrm{out}}$ is directly proportional to $2^{1,\mathrm{out}}$, which was shown above to be optimal when the resonance conditions (14) and (15) are fulfilled. Hence, the analysis of the out-of-phase first-order response $\mathfrak{O}^{1,\mathrm{out}}$ of the overall observable $O(t)$ allows for the selective and quantitative detection of a photoswitchable probe. Note that $\mathfrak{O}^{1,\mathrm{out}}$ can be easily extracted from the overall signal $O(t)$ *via* lock-in amplification, which enables to further improve the signal to noise ratio (see ESI†).

Out-of-phase response of the fluorescence intensity

Fluorescence emission is a particularly relevant observable to apply the present protocol.[44] In small molecules, combining fluorescence emission and photochromism is difficult since both processes are often competitive mechanisms for relaxation of the excited states.[45] In contrast, such a combination is widely found in photochromic fluorescent proteins which have recently led to powerful techniques including time-resolved protein tracking,[46] super-resolution microscopy[47–50] and high contrast imaging.[19,20] Moreover we recently showed that hybrid systems composed of a photoconvertible fluorogen that fluoresces upon binding to an acceptor provide an attractive two-component approach.[51]

Compared to other observables, the fluorescence intensity $I_F(t)$ includes an additional signal convolution since it is not only proportional to concentrations, but also proportional to the light intensity. Thus, considering that both concentrations of the states **1** and **2**, and light intensity are modulated, the fluorescence emission $I_F(t)$ can be written

$$I_F(t) = O(t)I(t) \tag{38}$$

with Q_i being the molecular brightness of **i**. In the general case of a periodic modulation of large amplitude, one obtains

$$I_F(t) = \mathfrak{I}^{\circ}_{\mathfrak{I}} + \sum_{n=1}^{\infty}\left[\mathfrak{I}^{n,\mathrm{in}}_{\mathfrak{I}} \sin(n\omega t) + \mathfrak{I}^{n,\mathrm{out}}_{\mathfrak{I}} \cos(n\omega t)\right]. \tag{39}$$

where (see ESI†)

$$\mathfrak{I}^{1,\mathrm{out}}_{\mathfrak{I}} = \alpha(Q_2 - Q_1)I^0\left[2^{1,\mathrm{out}} + g\left(2^{n,\mathrm{in}},\ 2^{n,\mathrm{out}}\right)\right] \tag{40}$$

with $n \geq 1$. For a sinusoidal or square wave modulation of small amplitude, $g(2^{n,\mathrm{in}}, 2^{n,\mathrm{out}}) = 0$ but it is non-vanishing in the case of a periodic modulation of large amplitude.

In a regime of sinusoidal or square wave modulation of small amplitude, the out-of-phase amplitude of the fluorescence emission, $\mathfrak{I}^{1,\mathrm{out}}_{\mathfrak{I}}$, is proportional to $2^{1,\mathrm{out}}$ and exhibits a resonant behavior. In contrast, such a conclusion cannot be directly drawn in the case of periodic modulation of large amplitude since analytical expressions are cumbersome. We therefore evaluated its relevance by means of numerical calculations using typical values found for photoswitchable fluorescent proteins.[52–56] To evaluate the possible interference originating from the second order term $g(2^{n,\mathrm{in}}, 2^{n,\mathrm{out}})$, we used eqn (40) to numerically compute the dependence of $\mathfrak{I}^{1,\mathrm{out}}_{\mathfrak{I}}$ on ω and I^0 (see ESI†). Hence we showed that the position and the amplitude of its optimum are similar independently on the nature and amplitude of the light modulation.

Therefore, the out-of-phase first-order fluorescence emission enables the selective and quantitative detection of a photoswitchable probe. Easily extracted from the overall signal $I_F(t)$ with the benefit of synchronous detection (see ESI†), it additionally provides an improved spatial resolution compared to usual fluorescence detection (see ESI†), which is an advantage for imaging.

Discussion

Our theoretical framework suggests that the out-of-phase first-order response to a periodically modulated light excitation under resonant conditions is appropriate to isolate the contribution of a photoswitchable probe of interest when the observable linearly depends on concentrations. Compared to a classical analysis that relies on an observation in absence of concentration modulation, this feature provides a simple protocol to perform selective and quantitative analyses in complex media without any preliminary separation.

A separation-free selective and quantitative analytical protocol

Instead of analyzing the behavior of a given photoswitchable probe upon varying the values of the control parameters I^0 and ω, we now examine which photoswitchable probe can be specifically addressed at fixed values of I^0 and ω.

Dynamic contrast. In a mixture of photoswitchable probes, dynamic contrast will originate from differences in the triplet of parameters (σ_{12}, σ_{21}, k^{Δ}_{21}). At fixed values of I^0 and ω, the optimized out-of-phase first-order response to a periodically modulated light excitation originates from matching (i) the rate constants for the thermally- and photochemically-driven

reactions (see eqn (14)) and (ii) the exchange relaxation time τ_{12}^0 with the radial frequency of the light modulation ω (see eqn (14) and (15)). We correspondingly use the (σ_{12} + σ_{21}, k_{21}^{Δ}) dynamic set to characterize the dynamic behavior of the photoswitchable probes illuminated at average intensity I^0 and radial frequency ω. Fig. 3a and b displays the dependence of the normalized in-phase $|1_{\text{norm}}^{1,\text{in}}| = |1^{1,\text{in}}/P_{\text{tot}}|$ and out-of-phase $|1_{\text{norm}}^{1,\text{out}}| = |1^{1,\text{out}}/P_{\text{tot}}|$ amplitudes on $(\sigma_{12} + \sigma_{21})I^0/\omega$ and k_{21}^{Δ}/ω for a weak sinusoidal light modulation. In contrast to the in-phase amplitude, the out-of-phase amplitude exhibits a single optimum centered on

$$\sigma_{12} + \sigma_{21} = \frac{\omega}{2I^0} \tag{41}$$

$$k_{21}^{\Delta} = \frac{\omega}{2}. \tag{42}$$

At fixed values of I^0 and ω, eqn (41) and (42) show that one can selectively isolate the contribution from the monodimensional $\left(\sigma_{12}, \frac{\omega}{2I^0} - \sigma_{12}, \frac{\omega}{2}\right)$ manifold in the three-dimensional (σ_{12}, σ_{21}, k_{21}^{Δ}) space of photoswitchable probes. Among the manifold members, the $|1_{\text{norm}}^{1,\text{out}}| = \sigma_{12}/[8(\sigma_{12} + \sigma_{21})]$ amplitude is ruled by the $\sigma_{12}/(\sigma_{12} + \sigma_{21})$ photochemical parameter. $|1_{\text{norm}}^{1,\text{out}}|$ is maximal $\left(\frac{1}{8}\right)$ for the $\left(\frac{\omega}{2I^0}, 0, \frac{\omega}{2}\right)$ photoswitchable probe. However the amplitude of all the manifold members notably remains of the same order of magnitude as long as σ_{12} does not drop much below the σ_{21} range.

Selective and quantitative detection. The above discussion shows that optimizing the out-of-phase response by choosing a couple (I^0, ω) that verifies the resonance conditions (14) and (15) opens an interesting way to selectively image and quantify a photoswitchable probe **P** in the presence of interfering compounds **X** (of total concentrations X_{tot}), each defined by a different set of parameters ($\sigma_{12,X}$, $\sigma_{21,X}$, $k_{21,X}^{\Delta}$). Note that **X** can be non-photoswitchable: in that case $\sigma_{12,X} = \sigma_{21,X} = 0$ and $k_{21,X}^{\Delta} = 0$. To illustrate this, we take a simplified case of a mixture containing photoswitchable probes, whose only the state **1** yields an observable signal, and possessing all the same brightness Q_1. In that case, a protocol relying on illumination at constant light intensity I^0 leads to a signal S^0 which is proportional to the sum of the contributions of the different probes such that:

$$S^0 \propto 1_P^0 + \sum_X 1_X^0 = \left(1_P^0/P_{\text{tot}}\right) P_{\text{titration}}^0 \tag{43}$$

where

$$P_{\text{titration}}^0 = P_{\text{tot}} + \sum_X \frac{\left(1_X^0/X_{\text{tot}}\right)}{\left(1_P^0/P_{\text{tot}}\right)} X_{\text{tot}} > P_{\text{tot}} \tag{44}$$

When the signal S^0 is used to titrate the concentration of **P** upon assuming that only the reactant of interest is present, the titration result $P_{\text{titration}}^0$ always overestimates the total concentration P_{tot} because of the contributions of the interfering compounds (see Fig. 4a).

In contrast, the corresponding out-of-phase first-order response to light modulation $\mathfrak{S}^{1,\text{out}}$

$$\mathfrak{S}^{1,\text{out}} \propto 1_P^{1,\text{out}} + \sum_X 1_X^{1,\text{out}} = \left(1_P^{1,\text{out}}/P_{\text{tot}}\right) P_{\text{titration}}^{1,\text{out}} \tag{45}$$

where

$$P_{\text{titration}}^{1,\text{out}} = P_{\text{tot}} + \sum_X \frac{\left(1_X^{1,\text{out}}/X_{\text{tot}}\right)}{\left(1_P^{1,\text{out}}/P_{\text{tot}}\right)} X_{\text{tot}} \tag{46}$$

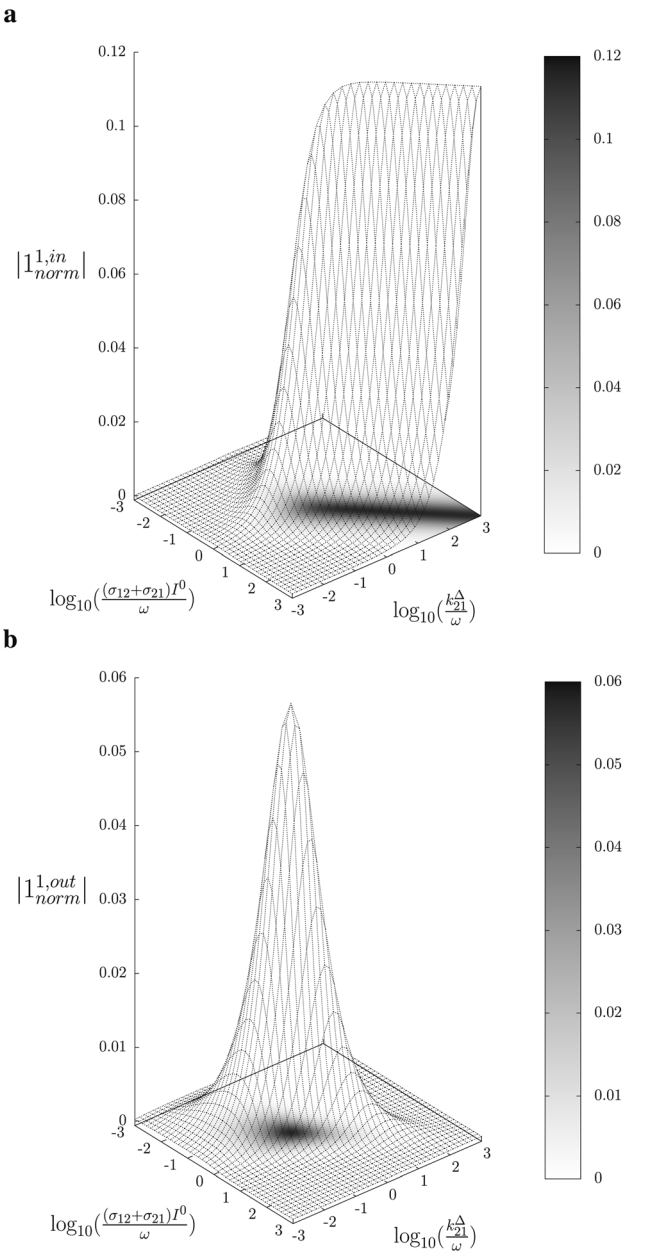

Fig. 3 Theoretical computation of the response of a photoswitchable probe **1** ⇄ **2** submitted to light harmonic forcing of small amplitude at fixed values of I^0 and ω. The normalized amplitudes of the in-phase and out-of-phase oscillations in **1** concentration, $|1_{\text{norm}}^{1,\text{in}}|$ (a) and $|1_{\text{norm}}^{1,\text{out}}|$ (b) respectively, are plotted *versus* $(\sigma_{12} + \sigma_{21})I^0/\omega$ and k_{21}^{Δ}/ω for $\sigma_{12}/(\sigma_{12} + \sigma_{21}) = 0.46$. See eqn (12) and (13).

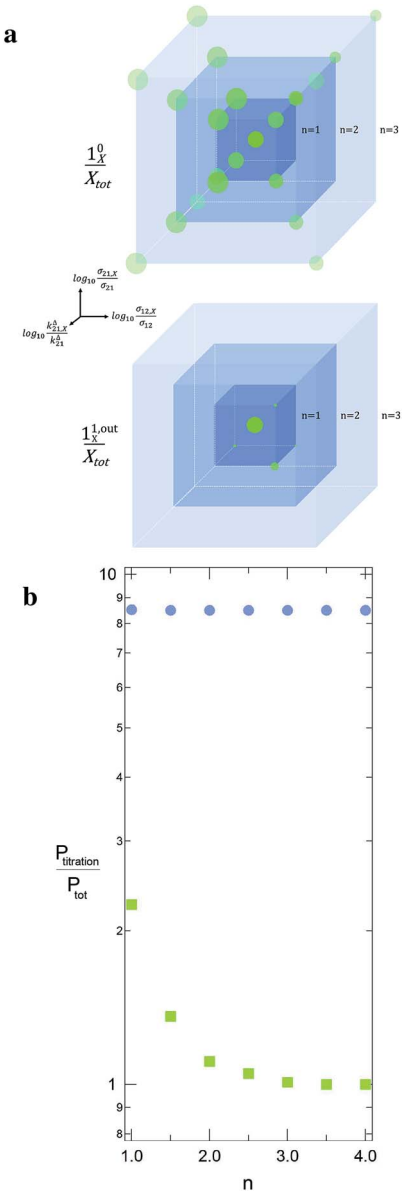

Fig. 4 Theoretical computation of $P_{titration}$ in seven different equimolar mixtures, which include the targeted triplet (σ_{12}, σ_{21}, k_{21}^{Δ}) plus eight other interfering ones. In each sample labelled n, the latter species correspond to the eight ($\sigma_{12,X}$, $\sigma_{21,X}$, $k_{21,X}^{\Delta}$) sets placed on the nodes of a cube centered on (σ_{12}, σ_{21}, k_{21}^{Δ}) and which mesh size is n in decimal logarithmic units (a; the individual responses ($1_X^0/X_{tot}$) and ($1_X^{1,out}/X_{tot}$) have been used to define the sphere radius associated to each ($\sigma_{12,X}$, $\sigma_{21,X}$, $k_{21,X}^{\Delta}$) set in ($1^0/P_{tot}$) and ($1^{1,out}/P_{tot}$) units). The n-dependence of the ratio of $P_{titration}$ to the effective target concentration P_{tot} is displayed in b for both the constant light intensity (disks) and the OPTIMAL (squares) methods. σ_{12} = 73 m^2 mol^{-1}, σ_{21} = 84 m^2 mol^{-1}, k_{21}^{Δ} = 1.5 × 10^{-2} s^{-1}; $I^0 = k_{21}^{\Delta}/(\sigma_{12} + \sigma_{21})$ = 9.6 × 10^{-5} ein s^{-1} m^{-2}, $\omega = 2k_{21}^{\Delta}$ = 3 × 10^{-2} rad s^{-1}.

enables to determine P_{tot} when the light parameters (I^0, ω) are tuned to the resonance conditions of **P**. Indeed, the term $1_P^{1,out}$ is then maximal while the terms $1_X^{1,out}$ are negligible (Fig. 3b). Thus, the signal from **P** now dominates those of the other probes, and the titration result $P_{titration}^{1,out}$ is approximatively equal to P_{tot} (see Fig. 4a). Fig. 4b illustrates for various mixtures the superiority of this second strategy over measurements performed at constant light intensity: whereas all the $P_{titration}^0$ are several times larger than the actual P_{tot} concentration, the discrepancy between $P_{titration}^{1,out}$ and P_{tot} becomes negligible as soon as (σ_{12}, σ_{21}, k_{21}^{Δ}) deviates from ($\sigma_{12,X}$, $\sigma_{21,X}$, $k_{21,X}^{\Delta}$).

Experimental implementation

This theoretical analysis suggests that it is possible to selectively and quantitatively visualize a given photoswitchable probe defined by the triplet of parameters (σ_{12}, σ_{21}, k_{21}^{Δ}) by simply analysing the out-of-phase (or quadrature-delayed) first-order component of the overall signal resulting from an illumination with a light of average intensity I^0 and periodically modulated at fundamental angular frequency ω so as to fulfil the resonance conditions (14) and (15) (Fig. 1).

To selectively address a photoswitchable probe of interest used for analyte labelling necessitates to preliminarily measure the sum of its molecular action cross-sections for photoisomerization $\sigma_{12} + \sigma_{21}$ and its thermal rate constant k_{21}^{Δ}, which can be easily performed, for instance, with a series of simple light jump experiments.[40,51] Once the parameters $\sigma_{12} + \sigma_{21}$ and k_{21}^{Δ} are known, one fixes the parameters I^0 and ω of the modulated illumination so as to fulfil the resonance conditions (14) and (15) of the photoswitchable probe. Then one extracts the out of phase first-order response $\Im^{1,out}$ from the acquired probe signal $S(t)$ (possibly contaminated by the contribution of interfering compound). One subsequently aims at extracting from $\Im^{1,out}$ the total probe concentration $P_{tot}^{1,out}$, which quantifies the labelled analyte. Although theoretical expressions could make possible to directly retrieve the concentrations of the photoswitchable probe from the observed signal, it is probably easier to proceed by calibration upon acquiring the signal from the pure photoswitchable probe at a reference concentration P_{tot}^{cal} under the same illumination conditions (see ESI†). Then

$$P_{tot}^{1,out} = \frac{\Im^{1,out}}{\Im^{1,out,cal}} P_{tot}^{cal} \quad (47)$$

When the photoswitchable probe is used as a titrating reagent, to fulfil the resonance conditions for the parameters I^0 and ω first requires an initial guess since the apparent molecular action cross-sections for photoisomerization and thermal rate constant now depend on the concentration of the targeted analyte A_{tot} (see ESI†). In fact, as usually encountered in any titration protocol, one should have an order of magnitude of the latter value before proceeding. Moreover, in contrast to the previous situation, the information sought for is not anymore P_{tot} but A_{tot}, which is contained in the amplitude of the **P** response to the light modulation (see ESI†). However, the latter amplitude is also proportional to P_{tot} and one has first to remove this dependence, for instance by relying on a ratiometric analysis, where one collects the overall signal upon adopting a same illumination but under two conditions of observation (*e.g.* by recording the fluorescence emission at two different wavelengths). Hence, the analyzed observable is now the ratio $\rho^{1,out} = \Im_1^{1,out}/\Im_2^{1,out}$ of the out-of-phase first-order

amplitudes of the signal collected under the two observation conditions (see ESI†). Calibration now requires to preliminarily investigate the dependence of $\rho^{1,\mathrm{out}}$ on A_{tot}. Then quantification can be simply achieved by recording the observable from a calibrating solution where the photoswitchable probe is used to sense a known concentration $A_{\mathrm{tot}}^{\mathrm{cal}}$. The concentrations of the analyte, which is retrieved at first-order, is eventually

$$A_{\mathrm{tot}}^{1,\mathrm{out}} = \frac{\rho^{1,\mathrm{out}}}{\rho^{1,\mathrm{out,cal}}} A_{\mathrm{tot}}^{\mathrm{cal}}. \quad (48)$$

Fields of application

The possibility to selectively and quantitatively retrieve the signal from a probe of interest without any separation is especially attractive when dealing with complex unknown systems.

Selective and quantitative detection in a mixture of probes. As a first field of application, one can think of selectively and quantitatively detecting a probe of interest in a system containing multiple probes or interfering compounds. This application could be especially useful in living cells, both to perform multiplexed observations as well as to overcome the contribution of endogenous components (Fig. 1a).

Selective and quantitative detection in a heterogeneous system. Another attractive field of application deals with the analysis or imaging of heterogenous systems. Indeed the brightness as well as the thermokinetic features of a probe often strongly depend on its environment. Thus, in a highly heterogeneous system (*e.g.* a living cell), it may be especially hazardous to retrieve a quantitative information from the probe signal acquired at constant illumination, when one has no information on the probe location. Indeed the collected signal depends on the concentration, the brightness and the thermokinetic features of the probe. In contrast, the out-of-phase first-order probe response strongly depends on the probe thermokinetic properties, which permits to selectively address the probe molecules located in a given phase, in which preliminary experiments for setting resonance conditions and calibration should have been performed. Therefore, the present analytical protocol could be fruitfully used to selectively analyze concentrations in a phase of interest within a multiphasic media (Fig. 1b), without requiring any extensive structural modification of the probe (as it is usually done to drive the probe location) or fluctuation-based protocols[57] to achieve calibration-free concentration measurements.

New challenges for probe development

The relevance and efficiency of the OPTIMAL/OPIOM protocols rely on the availability of appropriate photoswitchable probes. Many photoswitchable organic[58] as well as inorganic[59] platforms are presently available, so as to make promising the development of OPTIMAL labels with different types of observables. Moreover, these platforms have been already extensively implemented in the context of photocontrollable receptors,[60] so as to consider as well their use as OPTIMAL sensors. In the specific OPIOM context, photoswitchable fluorescent proteins are already highly significant probes. However, even in this case developing photoswitchable fluorescent probes fully optimised for OPIOM would enable to increase both the temporal resolution and the signal-to-noise ratio of this new imaging protocol. Indeed, although the above arguments are favorable, the extensive use of the OPTIMAL/OPIOM protocols may be hampered by the lack of a library of suitable engineered photoswitchable probes. This point has already motivated specific developments of photoswitchable fluorescent proteins in the context of SAFIRe.[61] In fact, most available reversibly photoswitchable fluorescent proteins (*e.g.* Dronpa[52]) have been engineered to exhibit extremely slow thermal return after photoconversion. In the context of OPIOM, such a feature is particularly detrimental in terms of fluorescence signal and temporal resolution: at resonance, intensity of light excitation as well as frequency of light modulation are proportional to the rate constant for thermal return (see eqn (14) and (15)). Even upon relying on the fastest Dronpa-3 mutant,[56] we only reached 20 s for the period of light modulation – typically leading to the minute range to record an image.[40] Such conditions are not optimal with respect to dynamic analysis of biological phenomena.[62] A slow thermal return also requires working at low average light intensity, which is not favorable to get a satisfactory signal to noise ratio.[48,63] We currently estimate that temporal resolution in the second range at a satisfactory few tens of W cm^{-2} average light power could be reached with photoswitchable probes exhibiting a relaxation time for thermal return in the 0.1–1 s range. Moreover, in relation to multiplex applications, Fig. 4 shows that it would be relevant to generate libraries of photoswitchable probes with values of their relevant dynamic parameters k_{21}^{Δ} and $\sigma_{12} + \sigma_{21}$ spread over at least two orders of magnitude ranges. Both photoswitchable fluorescent proteins as well as photoswitchable fluorescence turn-on probes are favorable candidates to implement such an engineering.[51,64,65]

Conclusion

By relying on the out-of-phase first-order response to periodic light modulation, OPTIMAL can discriminate – without any separation or washing step – a targeted photoswitchable probe among various interfering compounds, photoswitchable or not. Its experimental implementation is expected to be simple and cheap, just involving one-day preliminary investigations and appropriate tuning of two control parameters, the average intensity and the radial frequency of the modulated illumination, in order to fulfil robust resonance conditions. In particular, the OPTIMAL approach holds promises for selective and quantitative analyses in complex media such as encountered in biology: with optimized photoswitchable probes, the OPTIMAL protocol should make possible to titrate minor or signal-buried components as well as to facilitate multiplexed observations, as we recently demonstrated upon introducing the OPIOM fluorescence imaging approach in integral cells and organisms.[40]

References

1 C. M. Beck II, *Anal. Chem.*, 1994, **66**, 224A–239A.

2 J. A. Pérez-Bustamante, *Fresenius' J. Anal. Chem.*, 1997, **357**, 151–161.
3 D. Harvey, *Modern Analytical Chemistry*, McGraw-Hill, Boston, 2000.
4 T. R. Gingeras, R. Higuchi, L. J. Kricka, Y. M. D. Lo and C. T. Wittwer, *Clin. Chem.*, 2005, **51**, 661–671.
5 R. L. Nicholson, M. Welch, M. Ladlow and D. R. Spring, *ACS Chem. Biol.*, 2007, **2**, 24–30.
6 J. L. Duffner, P. A. Clemons and A. N. Koehler, *Curr. Opin. Chem. Biol.*, 2007, **11**, 74–82.
7 B. D. Bennett, E. H. Kimball, M. Gao, R. Osterhout, S. J. Van Dien and J. D. Rabinowitz, *Nat. Chem. Biol.*, 2009, **5**, 593–599.
8 B. Giepmans, S. Adams, M. Ellisman and R. Tsien, *Science*, 2006, **312**, 217–224.
9 B. Wu, K. D. Piatkevich, T. Lionnet, R. H. Singer and V. V. Verkhusha, *Curr. Opin. Cell Biol.*, 2011, **23**, 310–317.
10 R. Winkler-Oswatitsch and M. Eigen, *Angew. Chem., Int. Ed.*, 1979, **18**, 20–49.
11 M. Eigen and L. de Mayer, *Relaxation Methods in Techniques of Organic Chemistry*, Interscience Publishers, John Wiley and Sons, New York, London, 2nd edn, 1963, vol. VIII, pp. 895–1054.
12 H. Berthoumieux, C. Antoine and A. Lemarchand, *J. Chem. Phys.*, 2009, **131**, 084106.
13 H. Berthoumieux, L. Jullien and A. Lemarchand, *Phys. Rev. E: Stat., Nonlinear, Soft Matter Phys.*, 2007, **76**, 056112.
14 A. Lemarchand, H. Berthoumieux, L. Jullien and C. Gosse, *J. Phys. Chem. A*, 2012, **116**, 8455–8463.
15 F. Closa, C. Gosse, L. Jullien and A. Lemarchand, *J. Chem. Phys.*, 2013, **138**, 244109.
16 D. Baurecht and U. P. Fringeli, *Rev. Mod. Sci. Inst.*, 2001, **72**, 3782–3792.
17 I. Noda and Y. Osaki, *Two-Dimensional Spectroscopy Applications in Vibrational and Optical Spectroscopy*, Wiley, Chichester, 2004.
18 D. Boyer, P. Tamarat, A. Maali, B. Lounis and M. Orrit, *Science*, 2002, **297**, 1160–1163.
19 G. Marriott, S. Mao, T. Sakata, J. Ran, D. K. Jackson, C. Petchprayoon, T. J. Gomez, E. Warp, O. Tulyathan, H. L. Aaron, E. Y. Isacoff and Y. Yan, *Proc. Natl. Acad. Sci. U. S. A.*, 2008, **105**, 17789–17794.
20 Y. Yan, M. E. Marriott, C. Petchprayoon and G. Marriott, *Biochem. J.*, 2011, **433**, 411–422.
21 C. I. Richards, J.-C. Hsiang, D. Senapati, S. Patel, J. Yu, T. Vosch and R. M. Dickson, *J. Am. Chem. Soc.*, 2009, **131**, 4619–4621.
22 C. I. Richards, J.-C. Hsiang and R. M. Dickson, *J. Phys. Chem. B*, 2010, **114**, 660–665.
23 C. I. Richards, J.-C. Hsiang, A. M. Khalil, N. P. Hull and R. M. Dickson, *J. Am. Chem. Soc.*, 2010, **132**, 6318–6323.
24 C. Fan, J.-C. Hsiang, A. E. Jablonski and R. M. Dickson, *Chem. Sci.*, 2011, **2**, 1080–1085.
25 C. Fan, J.-C. Hsiang and R. M. Dickson, *ChemPhysChem*, 2012, **13**, 1023–1029.
26 A. E. Jablonski, J.-C. Hsiang, P. Bagchi, N. Hull, C. I. Richards, C. J. Fahrni and R. M. Dickson, *J. Phys. Chem. Lett.*, 2012, **3**, 3585–3591.
27 S. Sarkar, C. Fan, J.-C. Hsiang and R. M. Dickson, *J. Phys. Chem. A*, 2014, **117**, 9501–9509.
28 J.-C. Hsiang, A. E. Jablonski and R. M. Dickson, *Acc. Chem. Res.*, 2014, **47**, 1545–1554.
29 A. D. Q. Li, C. Zhan, D. Hu, W. Wan and J. Yao, *J. Am. Chem. Soc.*, 2011, **133**, 7628–7631.
30 Z. Tian, W. Wu, W. Wan and A. D. Q. Li, *J. Am. Chem. Soc.*, 2011, **133**, 16092–16100.
31 Z. Tian and A. D. Q. Li, *Acc. Chem. Res.*, 2013, **46**, 269–279.
32 H. Berthoumieux, C. Antoine, L. Jullien and A. Lemarchand, *Phys. Rev. E: Stat., Nonlinear, Soft Matter Phys.*, 2009, **79**, 021906.
33 I. Schoen, H. Krammer and D. Braun, *Proc. Natl. Acad. Sci. U. S. A.*, 2009, **106**, 21649–21654.
34 K. Zrelli, T. Barilero, E. Cavatore, H. Berthoumieux, T. Le Saux, V. Croquette, A. Lemarchand, C. Gosse and L. Jullien, *Anal. Chem.*, 2011, **83**, 2476–2484.
35 Q. Wei and A. Wei, *Chem.–Eur. J.*, 2011, **17**, 1080–1091.
36 L. Jullien, A. Lemarchand and H. Lemarchand, *J. Chem. Phys.*, 2000, **112**, 8293–8301.
37 D. Alcor, V. Croquette, L. Jullien and A. Lemarchand, *Proc. Natl. Acad. Sci. U. S. A.*, 2004, **101**, 8276–8280.
38 D. Alcor, J.-F. Allemand, E. Cogné-Laage, V. Croquette, F. Ferrage, L. Jullien, A. Kononov and A. Lemarchand, *J. Phys. Chem. B*, 2005, **109**, 1318–1328.
39 J. H. Scofield, *Am. J. Phys.*, 1994, **62**, 129–133.
40 J. Querard, T.-Z. Markus, M.-A. Plamont, C. Gauron, P. Wang, A. Espagne, M. Volovitch, S. Vriz, V. Croquette, A. Gautier, T. Le Saux and L. Jullien, *Angew. Chem., Int. Ed.*, 2015, **54**, 2633–2637.
41 G. Marriott, R. M. Clegg, D. J. Arndt-Jovin and T. M. Jovin, *Biophys. J.*, 1991, **60**, 1374–1387.
42 T. Sanden, G. Persson, P. Thyberg, H. Blom and J. Widengren, *Anal. Chem.*, 2007, **79**, 3330–3341.
43 J. Vogelsang, C. Steinhauer, C. Forthmann, I. H. Stein, B. Person-Skegro, T. Cordes and P. Tinnefeld, *ChemPhysChem*, 2010, **11**, 2475–2490.
44 B. Valeur, *Molecular fluorescence: principles and applications*, Wiley-VCH, 2001.
45 T. Fukaminato, *J. Photochem. Photobiol., C*, 2011, **12**, 177–208.
46 D. M. Chudakov, T. V. Chepurnykh, V. V. Belousov, S. Lukyanov and K. A. Lukyanov, *Traffic*, 2006, **7**, 1304–1310.
47 M. Fernandez-Suarez and A. Y. Ting, *Nat. Rev. Mol. Cell Biol.*, 2008, **9**, 929–943.
48 M. Hofmann, C. Eggeling, S. Jakobs and S. W. Hell, *Proc. Natl. Acad. Sci. U. S. A.*, 2005, **102**, 17565–17569.
49 E. Betzig, G. H. Patterson, R. Sougrat, O. W. Lindwasser, S. Olenych, J. S. Bonifacino, M. W. Davidson, J. Lippincott-Schwartz and H. F. Hess, *Science*, 2006, **313**, 1642–1645.
50 J. Lippincott-Schwartz and G. H. Patterson, *Trends Cell Biol.*, 2009, **19**, 555–565.
51 P. Wang, J. Querard, S. Maurin, S. S. Nath, T. Le Saux, A. Gautier and L. Jullien, *Chem. Sci.*, 2013, **4**, 2865–2873.
52 R. Ando, H. Mizuno and A. Miyawaki, *Science*, 2004, **306**, 1370–1373.

53 S. Habuchi, R. Ando, P. Dedecker, W. Verheijen, H. Mizuno, A. Miyawaki and J. Hofkens, *Proc. Natl. Acad. Sci. U. S. A.*, 2005, **102**, 9511–9516.
54 M. Andresen, A. C. Stiel, S. Trowitzsch, G. Weber, C. Eggeling, M. C. Wahl, S. W. Hell and S. Jakobs, *Proc. Natl. Acad. Sci. U. S. A.*, 2007, **104**, 13005–13009.
55 A. C. Stiel, S. Trowitzsch, G. Weber, M. Andresen, C. Eggeling, S. W. Hell, S. Jakobs and M. C. Wahl, *Biochem. J.*, 2007, **402**, 35–42.
56 R. Ando, C. Flors, H. Mizuno, J. Hofkens and A. Miyawaki, *Eur. Biophys. J.*, 2007, L97–L99.
57 S. Charier, A. Meglio, D. Alcor, E. Cogné-Laage, J.-F. Allemand, L. Jullien and A. Lemarchand, *J. Am. Chem. Soc.*, 2005, **127**, 15491–15505.
58 H. Bouas-Laurent and H. Dürr, *Pure Appl. Chem.*, 2001, **73**, 639–665.
59 M.-S. Wang, G. Xu, Z.-J. Zhang and G.-C. Guo, *Chem. Commun.*, 2010, **46**, 361–376.
60 M. Natali and S. Giordani, *Chem. Soc. Rev.*, 2012, **41**, 4010–4029.
61 A. E. Jablonski, R. B. Vegh, J.-C. Hsiang, B. Bommarius, Y.-C. Chen, K. M. Solntsev, A. S. Bommarius, L. M. Tolbert and R. M. Dickson, *J. Am. Chem. Soc.*, 2013, **135**, 16410–16417.
62 R. Milo, P. Jorgensen, U. Moran, G. Weber and G. M. Springer, *Nucleic Acids Res.*, 2010, **38**, D750–D753.
63 R. Y. Tsien, L. Ernst and A. Waggoner, *Fluorophores for Confocal Microscopy: Photophysics and Photochemistry*, Springer Science + Business Media, 3rd edn, 2006.
64 D. Bourgeois and V. Adam, *IUBMB Life*, 2012, **64**, 482–491.
65 X. X. Zhou and M. Z. Lin, *Curr. Opin. Chem. Biol.*, 2013, **17**, 682–690.